Mon. Not. R. Astron. Soc. **000**, 000–000 (0000) Printed 15 January 2004 (MN LATEX style file v2.2)

High-eccentricity trans-Neptunian objects as a source of Jupiter-family comets

V.V. Emel'yanenko[1], D.J. Asher[2] and M.E. Bailey[2]
[1] *South Ural University, Chelyabinsk, 454080, Russia*
[2] *Armagh Observatory, College Hill, Armagh, BT61 9DG*

Last update 2004 January 12; in original form 2003 November

ABSTRACT
The dynamical evolution of trans-Neptunian objects (TNOs) to the inner Solar system is investigated. The study is based on the observed sample of high-eccentricity TNOs with perihelia in the near-Neptune region, using a procedure to take account of observational biases. It is shown that observations favour TNOs in high-eccentricity orbits as the main source of Jupiter-family (JF) comets. The relative fraction of objects captured per year from the near-Neptune region to JF comets with perihelion distances $q < 1.5$ au is estimated as 0.2×10^{-10}. The maximum lifetime of typical JF comets with $q < 1.5$ au is approximately 200 revolutions. Based on the observed population of JF comets, there should be $\sim 10^{10}$ TNOs of cometary size in high-eccentricity orbits with $28 < q < 35.5$ au. If this population originated 4.5 Gyr ago, the primordial number must have been at least 20 times as large as the present one.

Key words: celestial mechanics – comets: general – Edgeworth-Kuiper belt – minor planets, asteroids – Solar system: formation.

1 INTRODUCTION

In recent years it has become widely accepted that the principal source of Jupiter-family (JF) comets is a flattened disc-like population of trans-Neptunian objects (TNOs) called the Kuiper or Edgeworth-Kuiper belt (Edgeworth 1943, Kuiper 1951), or simply the trans-Neptunian belt. The basic idea can be traced to papers such as Whipple (1964, 1972) and others, and especially Fernández (1980). However, despite the later work of investigators such as Duncan, Quinn & Tremaine (1988), Quinn, Tremaine & Duncan (1990), Duncan, Levison & Budd (1995), Duncan & Levison (1997) and Levison & Duncan (1997), there remains uncertainty as to the precise 'original' orbits of the Jupiter-family progenitors.

In fact, two qualitatively different scenarios have recently been suggested for the origin of JF comets, which in this paper we define by the value of the Tisserand parameter T with respect to Jupiter (Carusi & Valsecchi 1987). Thus, comets on short-period orbits (periods $P < 200$ yr) with perihelion distances within Jupiter's orbit and $T > 2$ are called JF comets. This allows us to compare our results with previous work on the observed and simulated characteristics of such comets (Fernández et al. 1999, Levison & Duncan 1997).

The first scenario focuses on the evolution of objects in relatively low-eccentricity orbits beyond Neptune, in the so-called Kuiper or Edgeworth-Kuiper belt (EKB). Here, following the argument developed by Levison & Duncan (1997), weak instabilities within the EKB provide a sufficient flux of objects on Neptune-encountering orbits to explain both the observed number and inclination distribution of JF comets (cf. Torbett & Smoluchowski 1990, Duncan et al. 1995). However, were this the case, with more than 800 TNOs discovered so far, this source — a dominant population of low-inclination, moderate-eccentricity orbits with perihelion distances close to the orbit of Neptune — should by now have been detected.

The contrast between expectations based on this picture and observations is illustrated in Figures 1 and 2. Figure 1 shows the relative rate of perihelion passages versus semimajor axis for an evolved population of particles in Neptune-approaching orbits ($28.4 < q < 31.9$ au) that began their evolution with perihelion distances distributed uniformly in the range (30,32) au and semimajor axes a distributed uniformly in the range (34,50) au. In the model, the initial inclinations were distributed between 0 and 40 degrees according to a sine law with a peak at 20°, and 3,000 particles were integrated for 4.5 Gyr including perturbations from the four outer planets.

As can be seen, in this model the majority of survivors on near-Neptune orbits are in mean-motion resonances with Neptune, but even considering just the non-resonant orbits we should still have discovered many more objects with semi-

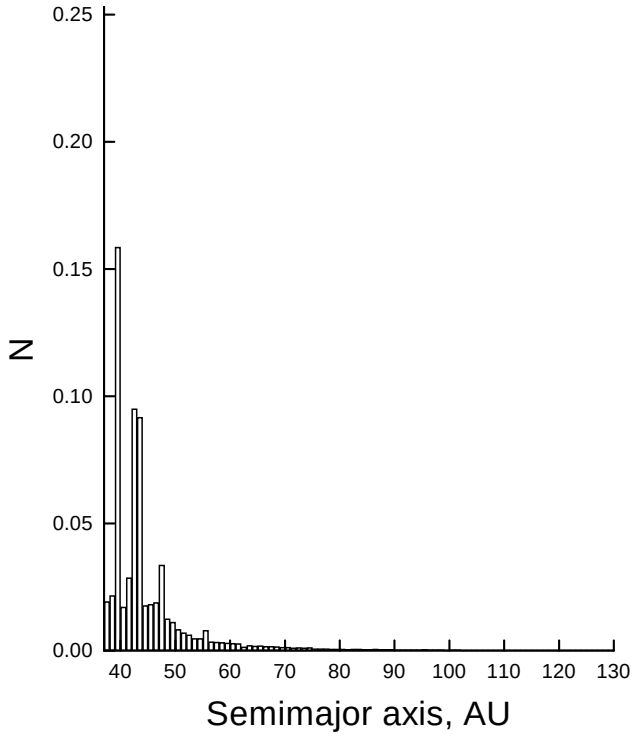

Figure 1. The relative steady-state frequency distribution of perihelion passages by particles with different semimajor axes, for an evolved population of objects in Neptune-approaching orbits ($28.4 < q < 31.9$ au). Initial perihelion distances and semimajor axes were uniform in (30,32) and (34,50) au respectively.

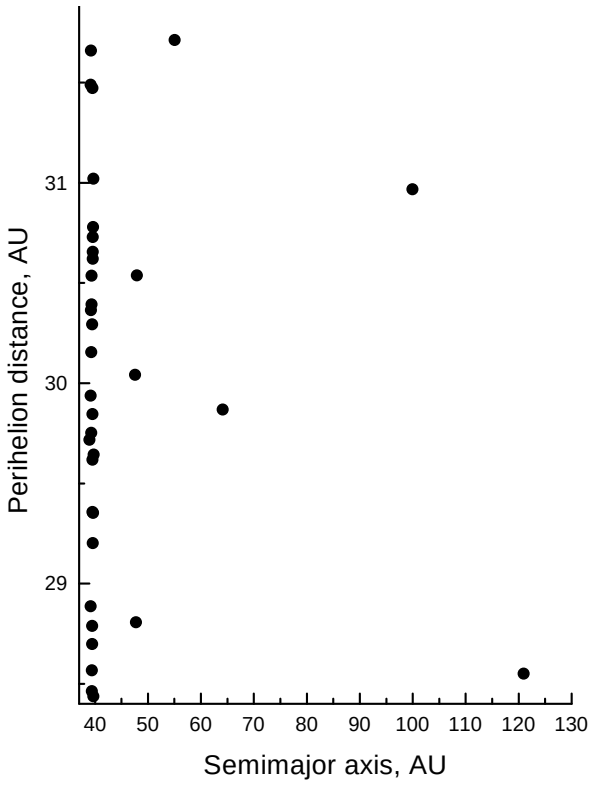

Figure 2. Observed distribution of perihelion distance and semimajor axis for multiple opposition objects in the near-Neptune region.

major axes in the range $40 < a < 50$ au than outside this region. As shown in Figure 2, the *observed* distribution of well-determined (i.e. multiple opposition) orbits with perihelion distances in the near-Neptune region has objects with much larger semimajor axes and higher eccentricities than predicted by this first model, and only those Edgeworth-Kuiper belt objects (EKOs) that move near the 2:3 and 1:2 mean-motion resonances with Neptune have perihelia close to or within Neptune's orbit. In fact, there is not a single observed example of an object with a perihelion distance near Neptune and semimajor axis in the EKB less than 50 au, apart from resonant objects.

It is impossible now to estimate reliably the relative rate of injection of resonant TNOs to the inner Solar system, owing to the large current uncertainties in their orbits. Some indirect conclusions, however, can be deduced from studies of resonant object dynamics. It is shown in Morbidelli (1997) and Nesvorny & Roig (2000) that, if the primordial population of resonant objects was distributed uniformly 4 Gyr ago, the current influx to unstable near-Neptune orbits from the main resonance 2:3 is smaller than from the classical EKB. Since the latter objects have not been discovered in the near-Neptune region, the contribution of resonant objects to JF comets would appear also to be relatively small. Nevertheless, although the final solution to this problem must await the determination of precise orbits for resonant TNOs, it is clear that the observed distribution of near-Neptune objects is very different from that predicted by a model in which the majority of JF comets originate from non-resonant EKB orbits (cf. Levison & Duncan 1997; Nesvorny & Roig 2000).

The second leading scenario (Duncan & Levison 1997) is that JF comets originate from a disc of scattered objects formed originally around the time of the accumulation of Neptune in the protoplanetary disc. Their simulation showed that a small fraction (∼1%) of the original objects survive to the present day in a so-called 'scattered disc'. This model also provided an explanation for the origin of TNOs in high-eccentricity orbits, which move far beyond the classical EKB. However, it has now been shown that the orbital distribution of observed high-eccentricity TNOs is not fully consistent with the scattered-disc model (Emel'yanenko 2002a; Emel'yanenko, Asher & Bailey 2003). Thus, high-eccentricity TNOs must either have a different source or the basic picture has to be modified.

Nevertheless, Figure 2 does provide evidence for TNOs in high-eccentricity orbits, and for these being a significant source of Neptune-approaching orbits. This paper therefore investigates the process by which such TNOs are captured into short-period JF comets. As noted above, the standard model for scattered disc objects (Duncan & Levison 1997) is not fully consistent with the observed orbital distribution. The differences cannot be explained by small number statistics. Since there is currently no theoretical model that fully describes the observed distribution for all TNOs in high-eccentricity orbits, we do not assume a particular model for the origin of these objects. Instead, we take as our starting point the *observed* sample of TNOs in high-eccentricity orbits with perihelia in the near-Neptune region. Although the number of reliable orbits is not large, such a sample provides a better estimate of the true orbital distribution of these objects than any current theoretical model, which would involve uncertain assumptions as to the formation of

the high-eccentricity population. In order to decrease statistical uncertainties we take account of observational biases, and finally compare the resulting distribution of short-period orbits with the known distribution of observed JF comets.

2 METHODS

2.1 Model

Previous work (Emel'yanenko et al. 2003) on the dynamics of TNOs in high-eccentricity orbits has shown that the rate of diffusion to the near-Neptune region is very slow for orbits with $q > 37$ au. Therefore, we have taken only objects with $q < 37$ au for the present investigation. Moreover, since a number of objects with $50 < a < 60$ au move close to the 2:5 resonance with Neptune (Emel'yanenko et al. 2003), and to avoid problems connected with the unknown stability of resonant objects (due to observational uncertainties), we have restricted our study also to initial $a > 60$ au.

For these reasons we selected a sample of multi-opposition TNOs with $a > 60$ au and $28 < q < 37$ au. In 2002 October we found 8 such objects in the list of the Minor Planet Center (MPC). Their perihelion distances range between 28.64 and 35.03 au. One object, namely 2000 YY_1, had a very uncertain orbit; therefore, we excluded this object from our investigation, leaving 7 'typical' high-eccentricity Neptune-approaching orbits as presented in Table 1. For each object, integrations were done of 250 orbits cloned by changing a uniformly within an interval $\pm\Delta a$ derived from the orbital uncertainty calculated by the MPC (cf. Emel'yanenko et al. 2003).

The main integrations were performed using the symplectic integrator described earlier (Emel'yanenko 2002b; Emel'yanenko et al. 2003). We included perturbations from the four outer planets, with the mass of the inner planets being added to to that of the Sun. In the region of the inner planets ($q < 2.5$ au), we used the RADAU integrator (Everhart 1985) from the MERCURY package (Chambers 1999), including directly the perturbations from seven planets, with Mercury's mass added to the Sun. The integrations were continued for 4.5 Gyr, unless the object collided with the Sun or planets, or evolved to $a > 1000$ au.

2.2 Observational biases

The observed objects represent populations with different orbital parameters and different chances of discovery. Therefore in comparing the results of this study with observed JF comets it is necessary to take account of observational biases in the discovered sample, which have various orbits $\mathbf{E} \equiv (a, e, i, \omega, \Omega)$ and apparent magnitudes m, and to weight the cloned orbits appropriately.

Let us assume that at any time the intrinsic size distribution of distant TNOs is independent of orbits, and it has a power law with index $-q'$, i.e.

$$f(\mathbf{E}, R)d\mathbf{E}dR = \Gamma n(\mathbf{E})R^{-q'}d\mathbf{E}dR, \quad (1)$$

where $n(\mathbf{E})$ is the orbit density function, R is the body's radius, and Γ is a constant. The probability p of discovery for an object with given values of $\mathbf{E}$ and m (as usual, this term refers to ranges $d\mathbf{E}$ and dm) is

$$p(m, \mathbf{E}) = p_0 p_1 p_2 p_3, \quad (2)$$

where p_0 is the probability that the object has orbital elements $\mathbf{E}$; p_1 is the probability that the object with orbital elements $\mathbf{E}$ falls within a field of surveys; p_2 is the probability that the object with orbital elements $\mathbf{E}$ has an apparent magnitude m in the field of surveys; p_3 is the probability of discovery for the object with the apparent magnitude m in the field of surveys. For the latter we assume that the detection of TNOs by surveys is biased by the brightness of the object but not by the orbital elements of the object. This assumption is similar to that used in the work of Trujillo & Brown (2001) on the radial distribution of the EKB.

The probability p_0 is determined by the number of objects with the orbital elements $\mathbf{E}$:

$$p_0 = C_0 n(\mathbf{E}), \quad (3)$$

where C_0 is a constant. We want our simulations to correspond, as far as possible, to objects from the true orbital element distribution, i.e. with particles weighted in proportion to p_0. On the other hand, the integrated clones are based on discovered objects, each of which exists with probability $p(m, \mathbf{E})$. Equation (2) therefore implies that in the comparison with observations each clone should be given a weight inversely proportional to $p_1 p_2 p_3$. The appropriate weights can be derived as follows.

TNO surveys target the ecliptic. Therefore, the field of surveys is concentrated within a very narrow range of ecliptic latitude β (Brown 2001; Trujillo, Jewitt & Luu 2001). Assuming a uniform distribution for the time of perihelion passage, the probability p_1 can be estimated as the fraction of time that the object spends in the small interval $\Delta\beta$:

$$p_1 = \frac{\Delta t}{P}, \quad (4)$$

where Δt is the time that the object moves in this interval, and P is the orbital period. Near $\beta = 0$

$$\Delta t \approx \frac{\Delta}{r\dot{v}\sin i}\Delta\beta, \quad (5)$$

where Δ and r are geocentric and heliocentric distances, respectively, and v is the true anomaly. In the astronomical system of units, for Keplerian motion

$$r\dot{v}P = \frac{2\pi a^2\sqrt{1-e^2}}{r}. \quad (6)$$

Therefore, we get approximately

$$p_1 = C_1\frac{r\Delta}{a^2\sin i\sqrt{1-e^2}}, \quad (7)$$

where C_1 is a constant.

To derive the probability p_2 we use Equation (1) for the distribution of R, and we assume zero phase angle (usually discoveries occur near opposition: $\Delta \approx r - 1$) and a constant albedo for all TNOs. These assumptions are the same as in the paper by Trujillo & Brown (2001) where it was shown that they are reasonable. The apparent magnitude m of the object at the moment of discovery in the field of surveys is approximately calculated by

$$m = H + 5\log(r\Delta), \quad (8)$$

Table 1. Heliocentric orbital elements at epoch 2002 Nov. 22.0 based on observations available up to the time we began our integration study.

	a	Δa	e	q	i	Ω	ω	M
2000 PJ_{30}	119.0	0.23	0.76	28.6	5.7	293.3	303.5	8.4
1999 RZ_{215}	100.4	2.93	0.69	31.0	25.5	341.6	336.4	1.4
2001 FZ_{173}	87.1	2.06	0.63	32.3	12.7	2.4	200.0	356.3
2001 KG_{77}	61.5	0.86	0.45	33.9	15.5	250.5	15.7	352.6
2001 FP_{185}	226.4	5.06	0.85	34.2	30.8	179.3	8.1	359.8
1999 CY_{118}	91.6	0.12	0.62	34.6	25.6	163.1	14.9	358.9
(15874) 1996 TL_{66}	84.3	0.10	0.58	35.0	24.0	217.8	184.9	0.6

Table 2. Data for the studied objects. The relative weights (Section 2.2) are each normalized to a mean of 1.00.

	w	w_1	w_2	w_3	H	m	r	Δ
2000 PJ_{30}	0.12	0.19	0.11	2.20	8.0	23.9	39.6	38.6
1999 RZ_{215}	0.15	1.06	0.14	0.38	7.8	22.6	31.0	30.1
2001 FZ_{173}	0.39	0.37	1.27	0.30	6.2	21.4	33.5	32.5
2001 KG_{77}	0.05	0.24	0.14	0.59	7.8	23.2	34.9	33.9
2001 FP_{185}	4.50	3.79	1.46	0.30	6.1	21.4	34.4	33.4
1999 CY_{118}	0.24	0.74	0.04	2.98	8.7	24.1	35.1	34.1
(15874) 1996 TL_{66}	1.54	0.61	3.84	0.25	5.4	20.8	35.3	34.3

where H is the absolute magnitude. From Equation (1) and the formula

$$H = A - 5\log(R), \tag{9}$$

where A is a constant, the density function ϕ of H is

$$\phi(H) = B10^{\alpha H}, \tag{10}$$

where $\alpha = (q'-1)/5$, and B is a constant. Using Equations (8) and (10), we obtain the expression for the density function ψ of m for objects with the orbital elements $\mathbf{E}$ in the field of surveys:

$$\psi(m) = \frac{B}{(r\Delta)^{5\alpha}}10^{\alpha m} = B10^{\alpha H}. \tag{11}$$

Then

$$p_2 = C_2 10^{\alpha H}, \tag{12}$$

where C_2 is a constant.

Using (3), (7) and (11), Equation (2) can be written in the form

$$p(m,\mathbf{E}) = \Lambda(\mathbf{E})10^{\alpha m}\epsilon(m), \tag{13}$$

where the orbit-dependent terms are collected in $\Lambda(\mathbf{E})$ and $\epsilon(m) = p_3$ is the discovery efficiency for a given value of m. To find $\epsilon(m)$ we apply a procedure which is similar to that employed in Trujillo & Brown (2001). Namely, we treat the estimate of $\epsilon(m)$ for any observed TNO with orbital elements $\mathbf{E}$ as an independent measurement. We use the data for all multi-opposition TNOs from the MPC list. The values $q' = 4$ and $\alpha = 0.6$ (Jewitt, Luu & Trujillo 1998; Trujillo et al. 2001; Gladman et al. 2001) are taken everywhere in this paper. We have obtained the following least-squares polynomial approximation in the range $20.8 < m < 24.2$:

$$p_3 = \epsilon(m) = C_3(2.92505 - 1.18782x - 1.05117x^2 +$$
$$+0.05912x^3 + 0.38372x^4 - 0.01634x^5 - 0.03445x^6), \tag{14}$$

where $x = m - 22.5$, and C_3 is a constant.

The estimate of the intrinsic orbital distribution $n(\mathbf{E})$ of distant TNOs is based on the observed objects from Table 1. Thus, we finally obtain a weighting factor w for each of our 7 typical high-eccentricity TNOs in Table 1:

$$w \propto w_1 w_2 w_3, \tag{15}$$

where the orbit factor $w_1 = 1/p_1$, the size factor $w_2 = 1/p_2$, and the apparent magnitude factor $w_3 = 1/p_3$. The relative weights and other data for the studied objects are given in Table 2 (here r, Δ and m correspond to the moment of discovery).

3 RESULTS

3.1 The rate of injection of Jupiter-family comets

We study the dynamical evolution to short-period orbits of TNOs with large semimajor axes and perihelia in the near-Neptune zone. The initial orbits are derived from the observed sample of TNOs with initial perihelion distances $28 < q < 35.5$ au and semimajor axes $60 < a < 1000$ au. We call this region the near-Neptune high-eccentricity (NNHE) region, and regard it as the proximate source of JF comets.

To describe the connection between the two different populations we assume (cf. Bailey et al. 1992) that the fraction of objects ejected from the NNHE region per unit time λ_{NN} is constant, so that the surviving number of NNHE objects is given by

$$\frac{dN_{NN}}{dt} = -\lambda_{NN}N_{NN}. \tag{16}$$

Consequently,

$$N_{NN}(t) = N_{NN}(0)\exp(-\lambda_{NN}t), \tag{17}$$

where $N_{NN}(t)$ is the number of NNHE objects at time t.

Furthermore, we assume that the fraction λ_{JF} of objects captured from the NNHE region to the JF region per unit time is also constant. Then the injection rate ν_{JF} of JF objects is

$$\nu_{JF} = \lambda_{JF}N_{NN} = \lambda_{JF}N_{NN}(0)\exp(-\lambda_{NN}t). \tag{18}$$

Our computations have shown that the change in the

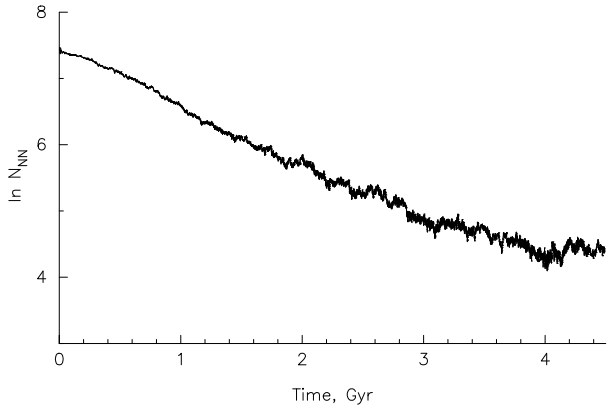

Figure 3. Resulting number of particles, weighted as in Equation (15) and shown on a log scale, in the near-Neptune high-eccentricity region as a function of time. The plot being close to a straight line suggests that the assumption of a constant fraction of objects ejected from the NNHE region per unit time is valid, and allows λ_{NN} to be estimated.

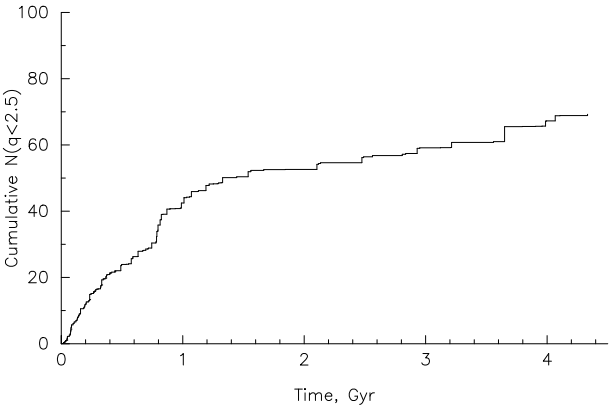

Figure 4. The cumulative number of particles, weighted as in Equation (15), captured to the JF region with $q < 2.5$ au as a function of time.

number of NNHE objects during the typical time for evolution of a captured object from the NNHE to the JF region is very small. Therefore we neglect these changes, and interpret our results as providing the instantaneous rate of injection of JF comets from a population of near-Neptune high-eccentricity orbits given by $N_{NN}(t)$.

Figures 3 and 4 show that both these assumptions are reasonable for the studied populations. Some discrepancy occurs after a few Gyr when the number of remaining NNHE objects in our sample becomes too small.

The steady-state number N_{JF} of JF comets originating from the NNHE region is then given by

$$N_{JF} = \nu_{JF} \bar{L}_{JF}, \tag{19}$$

where $\bar{L}_{JF}$ is the mean lifetime of JF comets in the defined region. From Equations (18) and (19)

$$\frac{N_{JF}}{N_{NN}} = \lambda_{JF} \bar{L}_{JF}. \tag{20}$$

Our results show that $\lambda_{NN} = 0.93 \times 10^{-9}\,\mathrm{yr}^{-1}$. For $q < 2.5$ au, $\lambda_{JF} = 0.36 \times 10^{-10}\,\mathrm{yr}^{-1}$, and for $q < 1.5$ au, $\lambda_{JF} = 0.18 \times 10^{-10}\,\mathrm{yr}^{-1}$. These values were calculated from least squares fits to data points (from our integrations) up to 2 Gyr, after which the data are increasingly sensitive to small number fluctuations. The lifetime of JF comets is estimated below.

3.2 The inclination distribution and lifetime of Jupiter-family comets

The distribution of inclinations is crucial for many aspects of the origin of JF comets. First, the low-i distribution of observed JF comets is the main argument against their direct capture from nearly parabolic orbits in the Oort cloud. Secondly, Levison & Duncan (1997) estimated the physical lifetime of JF comets with $q < 2.5$ au by comparing the calculated and observed inclination distributions. We use the same procedure in this work. However, Fernández et al. (1999) argued that most JF comets with $q < 2.5$ au have still not been discovered. Therefore we do not rely on this population, but instead compare our results with the i distribution for the JF population with $q < 1.5$ au, a sample which is almost complete (Fernández et al. 1999). We take the orbits of observed JF comets from Marsden & Williams (2003). There are 65 objects with $q < 1.5$ au and 169 objects with $q < 2.5$ au.

We investigate the consequences of assuming different values for the maximum lifetime L^*_{JF} of comets after their first entry into the region $q < 1.5$ au, $T > 2$. Our calculations confirm the result of Levison & Duncan (1997) that the i distribution of JF comets broadens with increasing L^*_{JF}. Fig. 5 shows the cumulative i distributions for observed comets and for our simulated objects for the values L^*_{JF}=1,200 yr and 12,000 yr. A Kolmogorov-Smirnov statistical test shows that the observed i distribution is best fit by L^*_{JF}=1,200 yr. In this case, the formal probability p_{KS} that the observations match the simulated distribution for $q < 1.5$ au is 0.999. The probability p_{KS} decreases rapidly if L^*_{JF} is changed, for example $p_{KS} = 0.1$ for L^*_{JF}=3,000 yr. Thus, the relatively narrow inclination distribution of observed JF comets sets a very tight constraint on their maximum lifetime in the observable region, with L^*_{JF} being much smaller than the mean dynamical lifetime in the same region ($\simeq$5,500 yr).

Applying the Kolmogorov-Smirnov test to JF comets with $q < 2.5$ au also shows that L^*_{JF} must be substantially less than the 12,000 yr estimated by Levison & Duncan (1997). For the i distributions of JF comets with $q < 2.5$ au, we have found that p_{KS} is practically unity if we assume that L^*_{JF} = 1,200 yr for $q < 1.5$ au and that L^*_{JF} is 2,000–3,000 yr for $q < 2.5$ au (in the latter case, the best value is 2,500 yr). Apart from the different methods of integration, we see two more possible reasons for the difference between our results and those of Levison & Duncan (1997). First, they used a very narrow distribution of initial inclinations for their assumed source orbits in the EKB, whereas our sample is based on real objects with a much wider range of initial inclinations. Secondly, they cloned objects after reaching the JF region. We do not know the details of their

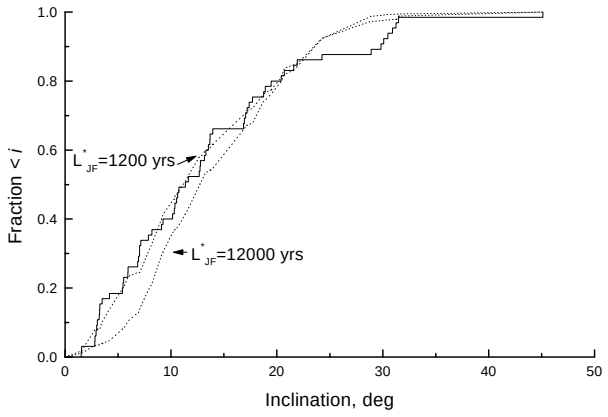

Figure 5. Solid line: inclination distribution of observed JF comets with $q < 1.5$ au. Dotted lines: simulated distributions assuming two different maximum lifetimes. Evidently $L^*_{JF} = 1,200$ gives a better fit to observations.

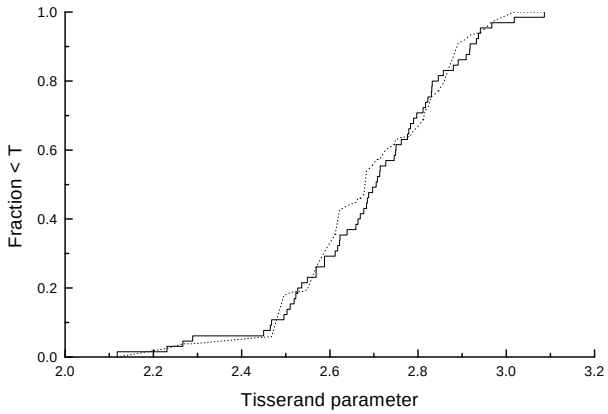

Figure 6. Observed (solid) and simulated (dotted) Tisserand parameter distributions of JF comets with $q < 1.5$, assuming $L^*_{JF} = 1,200$ yr.

cloning procedure, but we have found that such an approach can often produce too many resonant objects, i.e. a population with different dynamical properties from the sample it is meant to represent.

We have also compared the observed and predicted values of the Tisserand parameter T. Fig. 6 shows the distribution of T for JF comets with $q < 1.5$ au. The distribution from our simulation with L^*_{JF}=1,200 yr is also in good agreement with that observed.

3.3 The number of Jupiter-family comets and near-Neptune objects in high-eccentricity orbits

Finally, we estimate the present number of NNHE objects using Eq. (20). Our calculations give $\bar{L}_{JF}$=460 yr for $L^*_{JF} = 1,200$ yr in the region $q < 1.5$ au. From the data in Fernández et al. (1999), the total population of JF comets brighter than absolute nuclear magnitude H_N=18.5 (corresponding to a nuclear radius of ~ 0.7 km) and with $q < 1.5$ au is about 90. The corresponding number of NNHE objects with $60 < a < 1000$ au and $28 < q < 35.5$ au is then $\sim 10^{10}$. This figure is comparable to the number 0.4×10^{10} of scattered disc objects with q in the range 34–36 au estimated by extrapolation from the observed population of discovered TNOs (Trujillo, Jewitt & Luu 2000).

It is important to note, however, that the majority of TNOs in high-eccentricity orbits have perihelion distances larger than our NNHE objects (Emel'yanenko 2002a; Emel'yanenko et al. 2003), and so the total population of high-eccentricity TNOs estimated in this way is larger than 10^{10}.

Thus, according to our model, given 90 JF comets with $q < 1.5$ au, the number of JF comets with $q < 2.5$ au ranges from 230 (using the restriction $L^*_{JF} = 1,200$ yr for $q < 1.5$ au and $L^*_{JF} = 2,000$ yr for $q < 2.5$ au) to 1,000 (assuming $L^*_{JF} = 1,200$ yr for $q < 1.5$ au and no restriction for $q < 2.5$ au).

The restriction on the maximum lifetime of JF comets implies that many of them are inactive. According to our calculations, the mean dynamical lifetime of objects in the region $q < 1.5$ au, $T > 2$ is 5,500 yr. Therefore, the ratio of the total number of JF comets (both active and extinct) to that of active comets in this region is $5500/460 \approx 12$, although a number of authors (Bottke et al. 2002; Levison et al. 2002; Fernández, Gallardo & Brunini 2002) have argued that the real fraction of extinct comets is much smaller. Fernández et al. (2002) suggest that this can be explained by the quick disintegration of exhausted comets to meteoritic dust, although other models are also possible (Bailey 2002).

4 CONCLUSIONS

The principal conclusions of this study are the following:

(i) The observations favour TNOs in high-eccentricity orbits as the main source of JF comets.

(ii) If the near-Neptune high-eccentricity region ($60 < a < 1000$ au and $28 < q < 35.5$ au) is the dominant source of JF comets, there should be $\sim 10^{10}$ objects of cometary size ($R > 0.7$ km) in that region. The origin of such TNOs is not yet clear, but if this population formed 4.5 Gyr ago, the primordial number must have been at least 20 times as large as the present one.

(iii) The maximum lifetime of observed JF comets with $q < 1.5$ au captured from the NNHE region is surprisingly short, not exceeding ~ 200 revolutions. It is remarkable that this study should put the same severe restriction on their lifetime as for the lifetime of Halley-type comets in order to explain their observed number (Emel'yanenko & Bailey 1998). This again raises the important question of the fate of kilometre-size cometary nuclei.

ACKNOWLEDGMENTS

This research was supported by the Particle Physics and Astronomy Research Council and the Northern Ireland Department of Culture, Arts and Leisure. VVE thanks RFBR (Grant 01-02-16006), INTAS (Grant 00-240) and Armagh

Observatory for support during the course of this work. We thank Alessandro Morbidelli and an anonymous referee for helpful comments.

REFERENCES

Bailey M.E., 2002, Sci, 296, 2151
Bailey M.E., Chambers J.E., Hahn G., Scotti J., Tancredi G., 1992, in Brahic A., Gerard J.C., Surdej J., eds, Proc. 30th Liège Internat. Astrophys. Coll., Observations and Physical Properties of Small Solar System Bodies. Université de Liège, Liège, p. 285
Bottke W.F., Morbidelli A., Jedicke R., Petit J.-M., Levison H.F., Michel P., Metcalfe T.S., 2002, Icarus, 156, 399
Brown M.E., 2001, AJ, 121, 2804
Carusi A., Valsecchi G., 1987, in Ceplecha Z., Pecina P., eds, Interplanetary Matter. Czechoslovak Academy of Sciences, Ondrejov, p.21
Chambers J.E., 1999, MNRAS, 304, 793
Duncan M.J., Levison H.F., 1997, Sci, 276, 1670
Duncan M.J., Levison H.F., Budd S.M., 1995, AJ, 110, 3073
Duncan M., Quinn T., Tremaine S., 1988, ApJ, 328, L69
Edgeworth K.E., 1943, J. Brit. Astron. Assoc., 53, 181
Emel'yanenko V.V., 2002a, in Proceedings of Asteroids, Comets, Meteors (ACM2002). ESA Publications Division, Noordwijk, SP-500, p.327
Emel'yanenko V.V., 2002b, Cel. Mech. Dyn. Astron., 84, 331
Emel'yanenko V.V., Bailey M.E., 1998, MNRAS, 298, 212
Emel'yanenko V.V., Asher D.J., Bailey M.E., 2003, MNRAS, 338, 443
Everhart E., 1985 in Carusi A., Valsecchi G.B., eds, Dynamics of Comets: Their Origin and Evolution. Reidel, Dordrecht, p. 185
Fernández J.A., 1980, MNRAS, 192, 481
Fernández J.A., Tancredi G., Rickman H., Licandro J., 1999, A&A, 352, 327
Fernández J.A., Gallardo T., Brunini A., 2002, Icarus, 159, 358
Gladman B., Kavelaars J.J., Petit J.-M., Morbidelli A., Holman M.J., Loredo, T., 2001, AJ, 122, 1051
Jewitt D.C., Luu J.X., Trujillo C.A., 1998, AJ, 115, 2125
Kuiper G.P., 1951, in Hynek J.A., ed., Astrophysics – A Topical Symposium. McGraw-Hill, New York, p.357
Levison H.F., Duncan M.J., 1997, Icarus, 127, 13
Levison H.F., Morbidelli A., Dones L., Jedicke R., Wiegert P.A., Bottke W.F., 2002, Sci, 296, 2212
Marsden B.G., Williams G.V., 2003, Catalogue of Cometary Orbits 2003. Smithson. Astrophys. Obs., Cambridge, MA
Morbidelli A., 1997, Icarus, 127, 1
Nesvorny D., Roig F., 2000, Icarus, 148, 282
Quinn T., Tremaine S., Duncan M., 1990, ApJ, 355, 667
Torbett M.V., Smoluchowski R., 1990, Nat, 345, 49
Trujillo C.A., Brown M.E., 2001, ApJ, 554, L95
Trujillo C.A., Jewitt D.C., Luu J.X., 2000, ApJ, 529, L103
Trujillo C.A., Jewitt D.C., Luu J.X., 2001, AJ, 122, 457
Whipple F.L., 1964, Proc. Nat. Acad. Sci. USA, 51, 711
Whipple F.L., 1972, in Chebotarev G.A., Kazimirchak-Polonskaya E.I., Marsden B.G., eds, Proc. IAU Symp. 45, The Motion, Evolution of Orbits, and Origin of Comets. Reidel, Dordrecht, p. 401